Desalination and Water Treatment
www.deswater.com
doi: 10.5004/dwt.2021.27824

241 (2021) 135–145
November

Degradation of humic acid using a solar light-photocatalytic process with a $FeNi_3/SiO_2/TiO_2$ magnetic nanocomposite as the catalyst

Fatemeh Akbari[a], Maryam Khodadadi[b,*], Tariq J. Al-Musawi[c], Ibrahim Farouq Varouqa[d], Ali Naghizadeh[b]

[a]*Student Research Committee, Birjand University of Medical Sciences (BUMS), Birjand, Iran, email: fatemehakbari447@gmail.com*
[b]*Medical Toxicology and Drug Abuse Research Center (MTDRC), Birjand University of Medical Sciences (BUMS), Birjand, Iran, Tel. +98-915-562-3079; Fax: +98-56-32381661; emails: maryam.khodadadi@gmail.com (M. Khodadadi), al.naghizadeh@yahoo.com (A. Naghizadeh)*
[c]*Building and Construction Techniques Engineering Department, Al-Mustaqbal University College, 51001 Hillah, Babylon, Iraq, email: tariqjwad@yahoo.com*
[d]*Department of Civil Engineering, Faculty of Engineering, Isra University, Amman, Jordan, email: ibraheem.faroqa@iu.edu.jo*

Received 28 May 2021; Accepted 14 September 2021

ABSTRACT

The present study evaluates the degradation ability of $FeNi_3/SiO_2/TiO_2$ magnetic nanocomposite as a catalyst for degrading humic acid molecules in a photocatalytic process using simulated solar light-induced by light-emitting diode (LED) illumination. The morphology and structural properties of the used catalyst and the physiochemical factors influencing humic acid degradation (solution pH, catalyst dose, humic acid concentration, and reaction time) were examined in detail. In addition, the kinetics reaction type and mechanism of humic acid degradation were studied. Results showed that the suggested treatment method was efficient during the degradation of humic acid molecules, with non-toxic chemicals generated at the end of degradation, namely carbon dioxide and water. In addition, a degradation efficiency of 89% was achieved under optimal conditions. Compared with other similar methods, this study demonstrated that the interaction between $FeNi_3/SiO_2/TiO_2$ and LED solar light effectively degraded humic acid in an eco-friendly manner. The degradation reaction kinetics can be mathematically represented by a pseudo-first-order formula. The used catalyst can be recycled in the suggested treatment system six times with negligible losses in its degradation capacity. This study is necessary to understand how photocatalytic treatments using $FeNi_3/SiO_2/TiO_2$ magnetic nanocomposite particles can be applied for advanced wastewater purification of humic acid.

Keywords: Photocatalytic; $FeNi_3/SiO_2/TiO_2$; Solar light; Humic acid; Degradation efficiency; By-products

1. Introduction

At present, surface water contamination with organic pollutants is a significant problem globally. Organic compounds, such as humic acid, can cause significant harm to human health and aquatic life as these compounds tend to degrade into dangerous chemicals or produce disinfection by-products in aquatic environments. Human activities and natural factors can cause such compounds to enter the water resources [1,2]. Natural organic materials (NOMs) include materials derived from the decomposition activities of microorganisms, plants, and animals in the natural environment. As they can produce dangerous compounds, especially when they react with added chlorine, the presence

* Corresponding author.

of NOMs in drinking water treatment plants can cause direct harm and requires immediate solutions. Humic acids are NOM with hydrophobic properties [3,4]. The structure of humic materials consists of aromatic rings with carboxyl (–COOH) and hydroxyl (OH^-) functional groups. Humic acids have a higher potential for forming trihalomethane, which has hazardous characteristics and can change the odor, taste, and color of water when it is at a certain concentration [5]. In addition, trihalomethane can also attach to other pollutants in water, making it difficult to remove them [6]. Moreover, humic acids are also a carrier of disinfection by-products, as chlorine in water can combine with humic acid compounds, producing various products classified as carcinogenic [7]. Therefore, finding an efficient treatment method to remove humic acids from water is a scientific research priority in the drinking-water purification field.

Advanced oxidation has been strongly recommended as it is suitable for treating water/wastewater containing NOMs [2,8–10]. Photocatalytic processes are advanced oxidation methods that use light energy (such as UV and solar light) and metal oxides as a photocatalyst for the degradation of pollutants [11–13]. This method has been demonstrated as a low-energy, high-efficiency, and low-cost treatment, explaining its broad application [14,15]. Most importantly, this treatment is an environmentally-friendly technique as it can degrade toxic pollutants into ordinary by-products such as water, carbon dioxide, and minerals. Among photocatalyst materials, titanium dioxide (TiO_2) nanoparticles are considered to be the best, as they are generally non-volatile during exposure to light, relatively inexpensive, and have a high surface area and stable morphological properties. Moreover, these nanoparticles have high chemical stability and reactivity in a wide range of solution pH values [9,16,17].

Optical TiO_2 decomposition with solar radiation is a suitable process for organic pollutant degradation in wastewater. However, problems related to the separation and recycling of TiO_2 particles from the treated aqueous solutions prevents the wide application of this substance in treatment processes. One way to overcome this problem is to combine TiO_2 with magnetic particles such as Fe_3O_4. However, $FeNi_3$ magnetic nanoparticles used in photodegradation processes can be damaged by light exposure and can react with the generated by-products. Therefore, the addition of material between TiO_2 and Fe_3O_4 to protect $FeNi_3$ is important. SiO_2 particles, which can be easily prepared and are compatible with many materials, are promising candidates [18,19]. The formed magnetic nanocomposite particles (MNCPs) from a combination of TiO_2, SiO_2, and Fe_3O_4 ($FeNi_3/SiO_2/TiO_2$) are the focus of this study.

Khodadadi et al. [20], discussed humic acid degradation in detail using $FeNi_3/SiO_2/TiO_2$ MNCPs as a photocatalyst under ultraviolet (UV) radiation. However, the photocatalytic treatment process of humic acid wastewater using $FeNi_3/SiO_2/TiO_2$ MNCPs under solar light has not been extensively studied. Solar light is much safer than UV light, as it can be easily used without adverse effects on human health. Furthermore, treatments using solar light are more economical than those using UV radiation. In addition, using light-emitting diode (LED) bulbs with low energy consumption to simulate solar light can further reduce energy consumption in water treatment systems, preventing environmental pollution related to energy consumption [21,22]. Therefore, this study investigates the practical performance of a solar light photocatalytic process for the degradation of humic acid molecules in aqueous solutions. The removal efficiency of this pollutant was determined at various pH, initial humic acid concentrations, irradiation times, concentrations of H_2O_2, and concentrations of $FeNi_3/SiO_2/TiO_2$ MNCPs. This is important to determine the conditions with the maximum removal efficiency. Furthermore, an experiment was conducted to find the optimal degradation performance conditions using simulated solar light (using LED bulbs) and natural sunlight. Compared to the study by Khodadadi et al. [20], essential discussions regarding the characterization of $FeNi_3/SiO_2/TiO_2$ MNCPs is provided here.

2. Materials and methods

2.1. Chemicals

Analytical-grade humic acid stock solution (1,000 mg/L), ethanol, hydrazinium hydroxide ($N_2H_4{\cdot}H_2O$) with a purity of 80%, 2-isopropanol, nickel chloride ($NiCl_2{\cdot}6H_2O$), iron chloride ($FeCl_2{\cdot}4H_2O$), tetrabutyl orthotitanate (TBOT) ($Ti(OCH_2CH_2CH_2CH_3)_4$), and tetraethyl orthosilicate (TEOS) ($SiC_8H_{20}O_4$) were purchased from Sigma-Aldrich Co. (USA). In addition, the pH values of the working solutions were controlled by 0.1 N NaOH and HCl (Merck, Germany).

2.2. Synthesis of $FeNi_3/SiO_2/TiO_2$ MNCPs

$FeNi_3/SiO_2/TiO_2$ MNCPs was synthesized using coprecipitation and sol–gel methods based on the methodology documented in detail in the literature [20,23,24]. In addition, Fig. S1 is a schematic diagram of the experimental methodology adopted in this study for the synthesis of $FeNi_3/SiO_2/TiO_2$ MNCPs.

2.3. Characterization analyses

The microscopic specifications of the synthesized MNCPs were analyzed using transmission electron microscope (TEM) and field emission scanning electron microscopy (FESEM, SIGMA VP-500, ZEISS, Germany) images. In addition, the magnetic strength of the synthesized MNCPs was tested using a vibrating sample magnetometer (VSM, VSM 7400-S, Lake Shore Cryotronics Co., USA). Brunauer–Emmett–Teller (BET) and Barrett–Joyner–Halenda (BJH) analyses were performed to determine the pore size specifications and surface area of the catalyst using a high-precision BELSORP-MINI II analyzer (Microtrac Corp., Germany). To detect the functional groups of the used catalyst, the Fourier-transform infrared (FTIR) spectra of the prepared $FeNi_3/SiO_2/TiO_2$ MNCPs were recorded in a wavenumber range from 400 to 4,000 cm^{-1} (AVATAR spectroscope, USA). X-ray diffraction analysis was used to identify the crystal structure of the $FeNi_3/SiO_2/TiO_2$ magnetic nanoparticles. In addition, pH_{pzc} was determined according to the methodology presented in the [16,25] papers.

2.4. Photocatalytic experiments and calculations

The photocatalytic degradation process was performed using a STAR LED bulb (Afrough Company) as a solar light source with a wavelength of 450–500 nm, a 7 W power source, and average radiation intensity of 20 cm with intervals of 4,500 Lux. In addition, the humic acid degradation reaction was performed using a 250 mL quartz reactor filled with 150 mL humic acid solution placed on a shaker. The LED bulb, as a solar light emitter, was placed above the center of the reactor.

Before starting the radiation process of the humic acid solutions, the solutions were stirred in the dark for 10 min to reach the adsorption–desorption equilibrium. The net concentration of humic acid was determined by excluding the ratio of adsorbed concentration after reaction in the darkness. The remaining humic acid in the solution was considered as the initial concentration in the photocatalytic reactions. This step is important to avoid interference in the removal values from the two different processes of adsorption onto the catalyst surface and photodegradation reactions [18,24]. The efficiency of the used catalyst was tested at various pH (3, 5, 7, 9, and 11), $FeNi_3/SiO_2/TiO_2$ MNCP dosages (0.005–0.100 g/L), concentrations of humic acid (2, 5, 10, and 15 mg/L), and irradiation times (up to 200 min). During the photocatalytic reactions, 3 mL of liquid solution was collected at a predetermined time, and the residual humic acid concentration was measured using a UV-visible (UV-Vis) spectrophotometer (T80+ UV-Vis spectrophotometer, PG Instrument Ltd) at a spectral peak of 254 nm [26–28]. The initial and residual concentrations of humic acid were determined by comparing the calibration curves of the spectrophotometer absorbency measurements plotted according to the humic acid concentrations in the aqueous solution. The degradation efficiency (%R) was calculated as follows:

$$\text{Removal efficiency}\,(\%) = \frac{C_0 - C_r}{C_0} \times 100 \quad (1)$$

where C_0 and C_r (mg/L) are the initial (after 10 min reaction under dark conditions) and residual concentrations of humic acid in the aqueous solution.

3. Results and discussion

3.1. Characterization analysis

To determine the magnetic strength and properties of the used material, VSM analyses were applied on a sample of the $FeNi_3/SiO_2/TiO_2$ MNCPs, and its parent nanoparticles, that is, $FeNi_3$ and $FeNi_3/SiO_2$ (Fig. 1). The magnetic strength of the $FeNi_3/SiO_2/TiO_2$ MNCPs, $FeNi_3/SiO_2$, and $FeNi_3$ samples were determined as 17.560, 52.231, and 70.759 emu/g, respectively. These values indicate that the synthesized MNCPs formed from superparamagnetic particles and could therefore be separated from the aqueous solution by a magnet (Fig. 1). The high magnetic force of the used catalysts is highly desirable as it allows their separation from the water after treatment. As such, there is no need to use subsequent advanced techniques. However, the magnetic force values of $FeNi_3/SiO_2/TiO_2$ MNCPs were considerably lower than those of its parent nanoparticles. This is due to the coating of the $FeNi_3$ magnetite nanoparticles by SiO_2, followed by TiO_2.

As shown in the FESEM and TEM images (Fig. 2), the $FeNi_3/SiO_2/TiO_2$ MNCPs consist of several small particles, most of which are spherical, with diameters ranging from 20.10 to 33.50 nm. Most of these nanoparticles were grouped as aggregates; this is due to their magnetic properties, making them attractive to each other. In terms of compressibility, the $FeNi_3/SiO_2/TiO_2$ MNCPs is highly compressed, indicating its high density. In addition, Fig. 2 shows that the surface of this catalyst is amorphous and coarse. Furthermore, a number of small pores and cavities are present on the outer surface of the $FeNi_3/SiO_2/TiO_2$ MNCPs, demonstrating a porous structure of the used catalyst. These morphological properties of $FeNi_3/SiO_2/TiO_2$ MNCPs are favorable for photocatalytic degradation

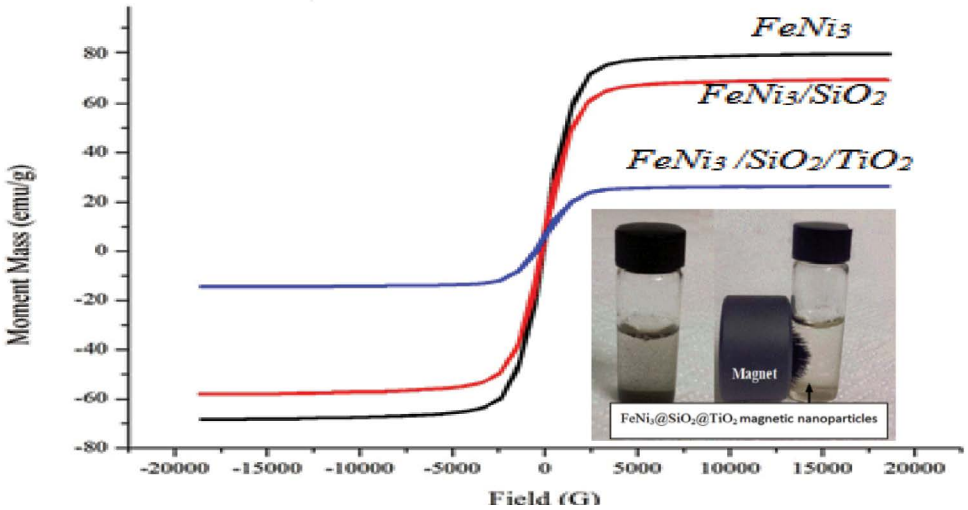

Fig. 1. VSM analysis of $FeNi_3$, $FeNi_3/SiO_2$, and $FeNi_3/SiO_2/TiO_2$ MNCPs, and two photos showing the behavior of the synthesized MNCPs before and after applying an external magnetic field.

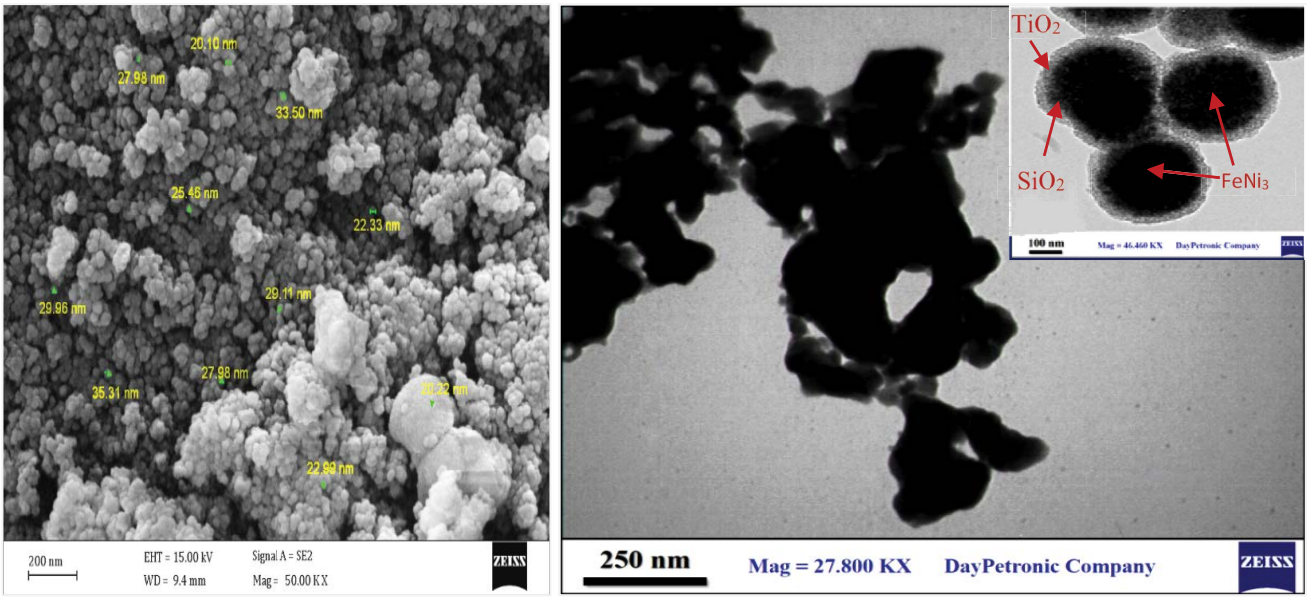

Fig. 2. FESEM and TEM images of the $FeNi_3/SiO_2/TiO_2$ MNCPs.

processes as they provide a high surface area, and thus, a large number of locations necessary for the reaction and adherence of pollutant molecules [29]. In the 100 nm scale TEM image, the light-colored outer layer represents TiO_2, as this material covered the inner $FeNi_3/SiO_2$ particles. In addition, the inner large dark circles are the core $FeNi_3$ magnetic particles, while the light gray layer between TiO_2 and $FeNi_3$ is due to SiO_2. Therefore, iron comprises the bulk of the $FeNi_3/SiO_2/TiO_2$ MNCPs.

The obtained FTIR spectra are depicted in Fig. 3. Comparisons of the FTIR spectra of $FeNi_3/SiO_2/TiO_2$ MNCPs detected after the synthesis and coating processes show that several peaks are similar, such as those detected at 470, 670–700, 800, 913, 970, 1,000–1,100, and 1,620 cm^{-1}. This indicates that the structure and the active groups of the synthesized catalyst were not altered, owing to the high thermal stability of the parental nanoparticles; thus, this catalyst is feasible for use in photocatalytic reactions. Peaks at 3,348 and 3,382 cm^{-1} are not apparent in the FTIR spectra of $FeNi_3/SiO_2/TiO_2$ MNCPs. This may be attributed to the titanium dioxide layer (outer shell) coating, which may reduce the transmittance values in the FTIR spectra of the covered metals. The peaks observed at approximately 460 to 480 cm^{-1} are related to the core material of $FeNi_3$ nanoparticles, indicating the Fe–Ni bond. The peaks at 531.75, 695.42, and 797.65 cm^{-1} are related to the O–Ti–O vibration group, indicating successful coverage of $FeNi_3/SiO_2$ by TiO_2 [20]. The two peaks at 913.61 and 1,031.52 cm^{-1} are due to the Ti–O–Si bending vibrations. The peaks observed at 1,638.99 and 1,124.05 cm^{-1} correspond to the SiO_2 group (Nasseh et al., 2020). Additionally, hydroxyl molecules appeared in the wavenumber range from 3,300 to 3,800 cm^{-1}. This group is attributed to the O-H stretching vibration of H_2O molecules, formed due to the dehydration process of the $FeNi_3/SiO_2/TiO_2$ MNCPs that may occur during the synthesis processes [23]. Notably, the 1,356.19 cm^{-1} peak in the FTIR spectra of $FeNi_3$ is related to the C–H stretching groups and appeared due to traces of organic matter used in the $FeNi_3$ synthesis process. For more details on these functional groups, please refer to [20].

BET analysis is important as the performance and efficiency of photocatalytic reactions for pollutant degradation depend on surface characteristics such as porosity and specific surface area. Therefore, BET analysis was conducted on a sample of $FeNi_3/SiO_2/TiO_2$ MNCPs. The results of this analysis are presented in Fig. 4. The determined specific surface area, mean pore volume, and pore diameter values of the $FeNi_3/SiO_2/TiO_2$ MNCPs were 177.58 m^2/g, 0.3876 cm^3/g, and 8.7374 nm, respectively. These characterization values are favorable in light of the tested material in the photocatalytic reactions. In other words, the high surface area of the photocatalyst indicates that more reaction sites are available for the interaction between the catalyst particles and pollutant molecules, thus facilitating photocatalytic reactions [16,30]. These characterization results provide the first evidence for $FeNi_3/SiO_2/TiO_2$ MNCPs as a high-performance photocatalyst in photocatalytic treatment systems. The isotherm shown in Fig. 4 is a typical type-IV isotherm with a well-defined hysteresis loop with a relative pressure range of 0.3–1, which suggests the porous structure catalyst.

3.2. Effects of various parameters

3.2.1. Solution pH

In this experiment, the performance of the photocatalytic treatment of humic acids was investigated under acidic and basic pH values of 3, 5, 7, 9, and 11; the results are presented in Fig. 5. The other parameters were set at constant values, as shown in the caption of Fig. 5. It can be concluded that an increase in pH values has a negative impact on the humic acid degradation efficiency (Fig. 5a). The degradation efficiency decreased significantly from

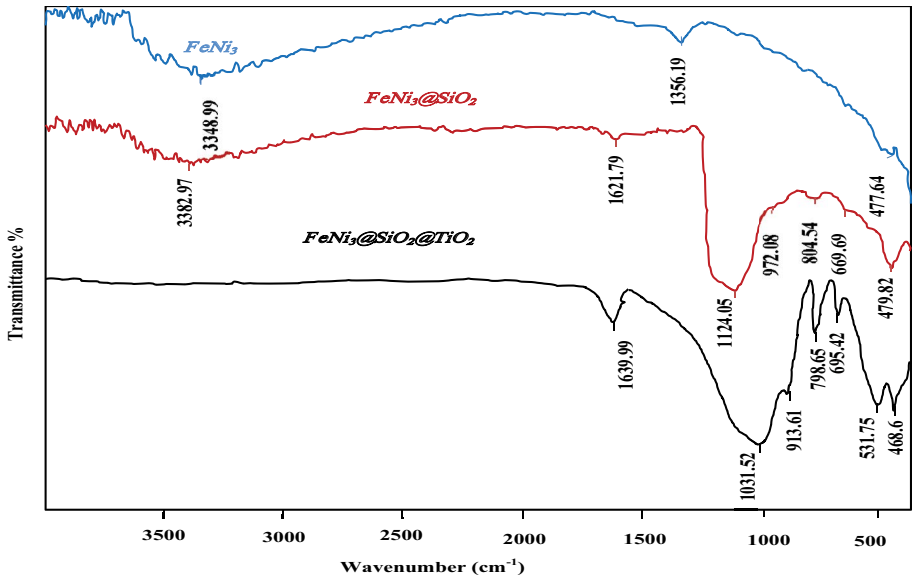

Fig. 3. FTIR spectra of $FeNi_3/SiO_2/TiO_2$ $MNCP_S$ and its parent nanoparticles.

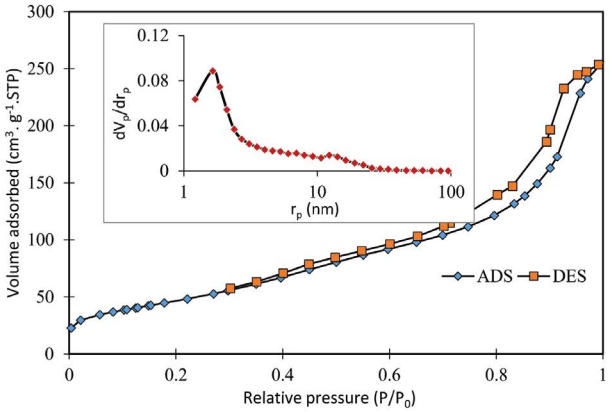

Fig. 4. N_2 adsorption–desorption isotherm plots of Brunauer–Emmett–Teller (BET) analysis combined with Barrett–Joyner–Halenda (BJH) isotherm plot of $FeNi_3/SiO_2/TiO_2$ MNCPs; here r_p and V_p denote pore radius and pore volume, respectively.

89.53% to 22.16% as the solution pH increased from 3 to 7. Then, it further decreased as pH increased, reaching the lowest value at pH 11. This high degradation efficiency phenomenon at low pH values can be explained by the following reasons. The first is the conversion of H^+ to $H^•$ at acidic pH values, resulting in the production of radical molecules with a high degradation ability [31,32]. The production of these radicals enhances the degradation rate of organic pollutants in photodegradation reactions. The second reason is that, as the pH_{pzc} characterization parameter of the $FeNi_3/SiO_2/TiO_2$ MNCPs is approximately 7.9 (Fig. 5b), the surface of the MNCPs is covered by positive charges at pH < pH_{pzc} and vice versa. On the other hand, humic acid has an anionic structure, with electrostatic attraction at the positive sites of $FeNi_3/SiO_2/TiO_2$ MNCPs in acidic mediums. The attraction between the humic acid molecules and photocatalyst particles, accelerates the contact between them in an aqueous solution, increasing the possibility of humic acid degradation [24]. The degradation efficiency was low (below 20%) at pH > 7; this is attributable to the accumulation of negative charges (OH^-) at such pH values. Under these circumstances, the repulsion force between the photocatalyst particles and humic acid molecules is stronger as the pH increases, leading to a decrease in the reaction rate. Thus, low degradation efficiencies are presented in Fig. 5. A similar trend of degradation efficiencies was also determined in two similar previous studies that examined the photodegradation process of a tetracycline antibiotic, tamoxifen drug, and humic acid [16,20].

3.2.2. Initial concentration

In this study, the photocatalytic process of humic acid degradation by $FeNi_3/SiO_2/TiO_2$ MNCPs was investigated at the initial concentration range of 2–15 mg/L, whereas the other conditions were fixed at pH = 3 and $FeNi_3/SiO_2/TiO_2$ MNCP dose = 0.1 g/L. Furthermore, the irradiation in the photocatalytic reaction was continued for 200 min. The results of this experiment (Fig. 6a) indicate that when the concentration was increased from 2 to 5 mg/L, the degradation efficiency of humic acid increased from 45.99% to 61.70%. Thereafter, the increase in the humic acid concentration up to 15 mg/L led to a 15% decrease in the maximum degradation efficiency. The increase in the degradation efficiency at the beginning is attributable to the availability of optimal conditions for the degradation of this concentration of pollutant, especially related to the photocatalytic dosage. As previously shown, the amount of photocatalyst used in the aqueous solution has a direct effect on the degradation process, as it provides the most important parameter in the degradation reaction, the reaction sites. As the humic acid concentration increases with the fixed value of the photocatalytic dose, the degradation of this pollutant decreases

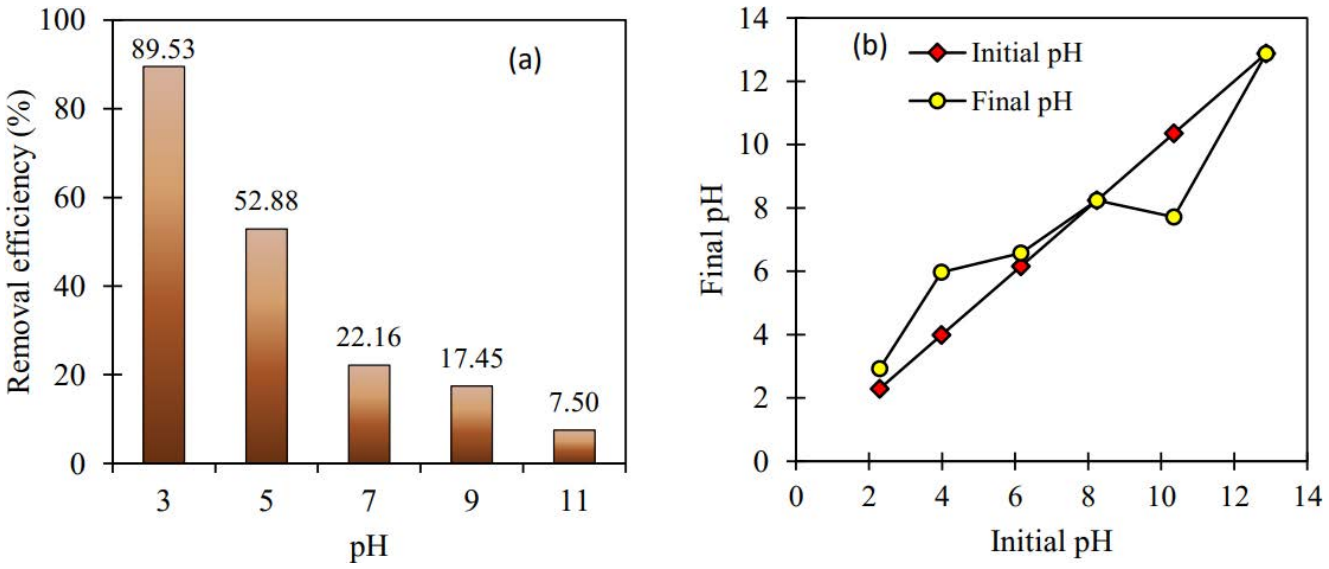

Fig. 5. Results of the pH effect study; (a) effect of pH on the humic acid degradation efficiency ($FeNi_3/SiO_2/TiO_2$ MNCPs dose = 0.03 g/L, initial humic acid concentration = 5 mg/L, irradiation time = 120 min, and temperature at 25°C); (b) pH_{pzc} analysis.

as the increasing concentration leads to an increase in the pollutant molecules in the solution. Thus, the adsorption of these molecules onto photocatalytic particles also increases. The accumulation onto the photocatalyst particles impedes the direct penetration of solar light to the photocatalytic particles, restricting the photocatalytic reaction [33].

3.2.3. $FeNi_3/SiO_2/TiO_2$ MNCPs dose and irradiation time

The effect of increasing the photocatalyst dose on the degradation of humic acid was studied in the range 0.005–0.1 g/L. This experiment was conducted under the following conditions: pH = 3 (the optimal value as found from previous experience), humic acid concentration = 5 mg/L, irradiation time = up to 200 min, and temperature = 25°C. The results are shown in Fig. 6b. When the $FeNi_3/SiO_2/TiO_2$ MNCP dose increased to 0.03 g/L, the removal efficiency increased. This is because the increase in the amount of catalyst leads to more reaction sites for the degradation of pollutant molecules during the photocatalytic treatment. Thus, the increase in reaction sites is beneficial for improving the degradation rate. On the other hand, further increases in the dose of the $FeNi_3/SiO_2/TiO_2$ MNCPs led to a negative effect on humic acid degradation. This abnormal result in the treatment system can be explained as an increase in the photocatalyst quantity in the aqueous solution led to increased turbidity. The increase in turbidity obstructs the penetration of light into the solution, ultimately hampering the photocatalytic reaction [34]. In other words, solar radiation is responsible for electron excitation on the TiO_2 layer of $FeNi_3/SiO_2/TiO_2$ MNCPs. This process leads to the production of free radicals that possess strong activity for oxidizing organic pollutants [8,11]. Therefore, the absorption or reflection of solar light by any impurities generates fewer radicals in the photocatalytic system [35].

Fig. 6a and b simultaneously show the variation in the degradation efficiency as a function of irradiation time up to 200 min. The degradation efficiency of humic acid increased from 7.22% to 61.51% upon increasing the exposure time to 120 min (Fig. 6a, curve of 5 mg/L). Under all conditions, an irradiation time of 120 min is adequate to reach the equilibrium state of the degradation process. Further increases in the irradiation time above 120 min did not significantly alter the removal efficiency for any case. A treatment process that comprises a short equilibrium time of 120 min is considered favorable for practical applications [30].

3.2.4. $FeNi_3/SiO_2/TiO_2$ and different sources of irradiation

This study comparatively examined the effects of the source light on humic acid degradation efficiency with and without the $FeNi_3/SiO_2/TiO_2$ MNCP photocatalyst material; that is, photocatalytic and photolysis processes, respectively. For this purpose, three additional experiments for the degradation of humic acid were conducted under the same conditions (pH = 3, initial pollutant concentration = 5 mg/L, photocatalyst dose (if applicable) = 0.03 g/L, and irradiation/reaction time up to 120 min) to accomplish the following processes: (i) photocatalytic process using natural sunlight, (ii) photolysis using natural sunlight, and (iii) photolysis using simulated solar light generated by LED bulbs. The results of these three experiments are plotted in the same graph with the photocatalytic data of Fig. 6a (curve of 5 mg/L), the results are presented in Fig. 7. Comparing the four curves in this figure illustrates that the photocatalytic process using LED-generated solar light was the most efficient for degrading humic acid molecules. Thus, the degradation efficiencies at the equilibrium state can be ranked for the four different processes as photocatalytic using LED solar light (89.5%) > photolysis using LED solar light (30.3%) > photocatalytic using sunlight (20.2%) > photolysis using sunlight (14.2%). This finding highlights the role of photocatalyzers such as $FeNi_3/SiO_2/TiO_2$ MNCPs in the photocatalytic

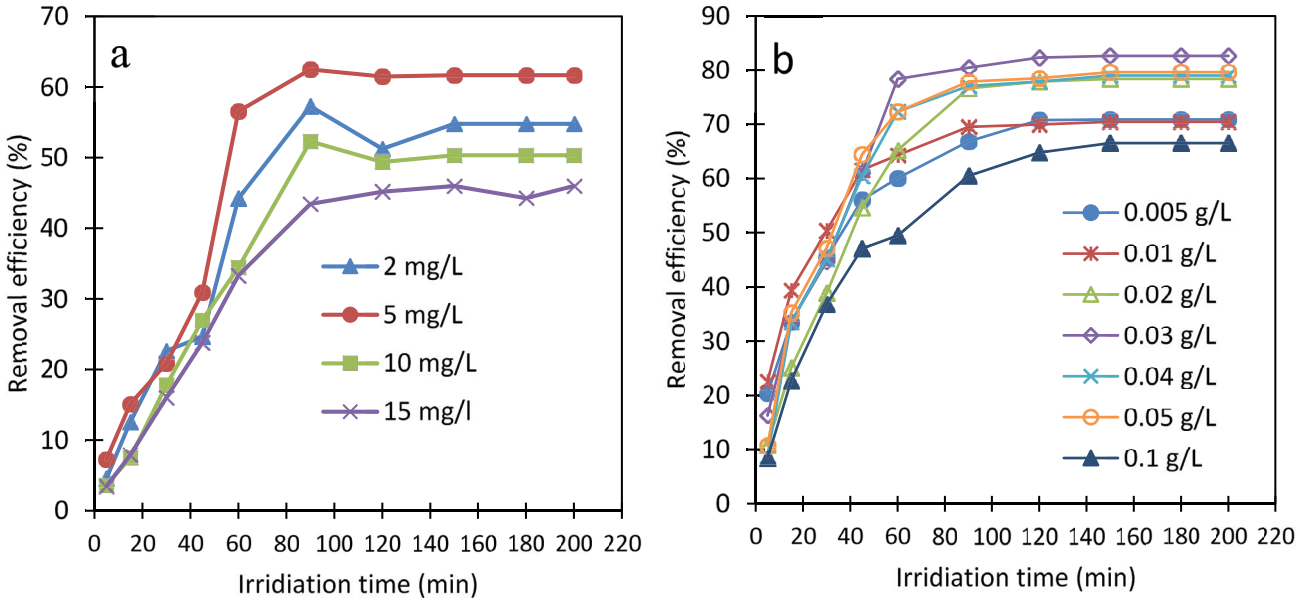

Fig. 6. (a) Effect of the initial humic acid concentration (pH = 3, $FeNi_3/SiO_2/TiO_2$ MNCPs dose = 0.03 g/L, irradiation time = 120 min, and temperature = 25°C), and (b) effect of the $FeNi_3/SiO_2/TiO_2$ MNCPs dose (pH = 3, initial humic acid concentration = 5 mg/L, irradiation time = 120 min, and temperature = 25°C).

treatment system. Moreover, the process comprises solar light generated by the LED, which is more efficient than the sunlight. This is because the solar light-induced by LED bulbs is stronger than natural sunlight [27,36]. Therefore, its ability to degrade organic pollutants in the photocatalytic treatment process is better. As shown in Fig. 7, after 45 min of reaction time, the degradation efficiency decreased when using natural solar light. The reason for this phenomenon is that during exposure to sunlight, the specimens evaporate after a specific time; as a result, the volume of the samples reduces [16,37]. As a result, the removal efficiency determined from photolysis using LED solar light at equilibrium state was higher than the value given from photocatalytic using sunlight.

3.3. Photocatalytic process mechanism

In this study, the possible reactions and pathways of humic acid degradation in the solar light photocatalytic reaction using $FeNi_3/SiO_2/TiO_2$ MNCPs was investigated. First, it should be noted that the TiO_2 nanoparticles show high photocatalytic performances for the degradation of various organic pollutants. During photocatalytic reactions using the catalyst containing TiO_2 nanoparticles applied in this work, the catalyst particles initially have a full valence band (VB), an empty conduction band (CB), and absorb light. Accordingly, when the light energy (from the LED bulb in this study) is greater than or equal to the band-gap level, it can transfer electrons from the base (i.e., VB level) to an excited state, ultimately elevating them to the CB level. This process creates an electron cavity that has a positive hole charge (h^+) and negative electron (e^-), which in turn oxidize O_2 and H_2O molecules, yielding both $^{\bullet}O_2^-$ and ^-OH highly active radicals [34,38]. The reaction that produce these free radicals as the main spices ($^{\bullet}O_2^-$ and ^-OH) for photocatalytic degradation are shown in the following equations (Khodadadi et al. [20]).

It is supposed that the interaction of generated free radicals with the humic acid molecules will not able to full mineralization of this pollutant unless through the formation of intermediate compounds. In fact, the continual presence of $^{\bullet}OH$ and O_2^- radicals in the aqueous solution will lead to degrade and convert the organic matter to non-toxic by-products of CO_2 and H_2O [Eqs. (2) and (3) [20,39]. Therefore, the solar light degradation process using $FeNi_3/SiO_2/TiO_2$ MNCPs is a clean and eco-friendly process for the treatment of humic acid-loaded wastewater. The detailed mechanism of the applied solar light photocatalytic treatment system of humic acid using $FeNi_3/SiO_2/TiO_2$ MNCPs is depicted in Fig. S2. However, the nature of the intermediate compounds generated from the treatment system should be taken into consideration in future studies.

$$^{\bullet}OH + \text{humic acid} \rightarrow \text{Intermediate compounds} \rightarrow CO_2 + H_2O \quad (2)$$

$$O_2^- + \text{humic acid} \rightarrow \text{Intermediate compounds} \rightarrow CO_2 + H_2O \quad (3)$$

3.4. Kinetics study

Determining the pollutant degradation kinetics in the photocatalytic process is important. To accomplish this, the kinetic data are analyzed with pseudo-first-order kinetics [Eq. (2)] [20,32]. This was achieved by plotting the humic acid photodegradation data in Fig. 6a, namely $\ln(C_0/C_t)$ as a function of irradiation time (t) in the range of 0 to 200 min, as depicted in Fig. 8.

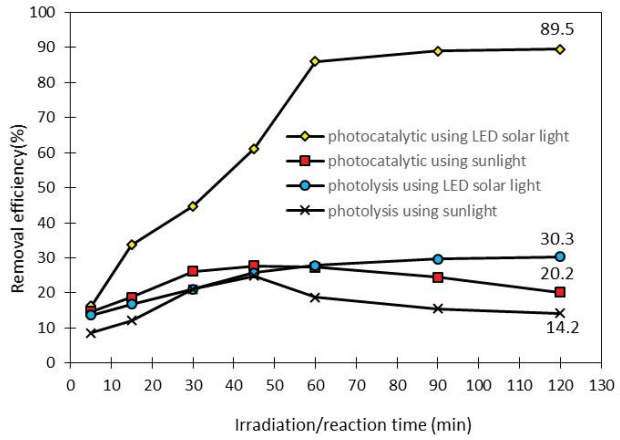

Fig. 7. Comparison of the humic acid degradation efficiencies from the application of photocatalysis and photolysis processes.

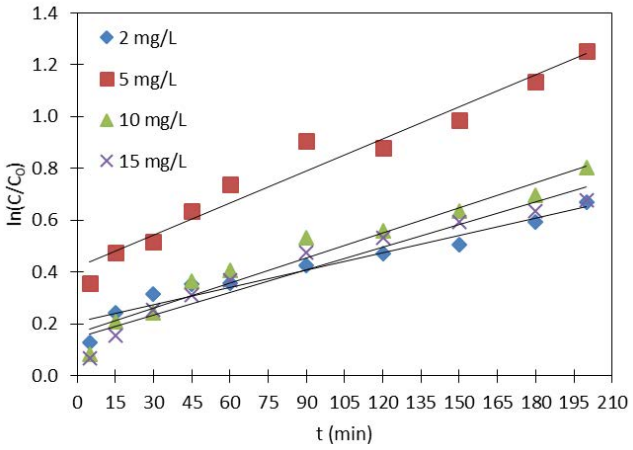

Fig. 8. Linear plot for $\ln(C/C_0)$ vs. t to determine the reaction kinetics.

$$\ln\left(\frac{C_r}{C_0}\right) = -k_{obs}t \quad (4)$$

where k_{obs} (min^{-1}) is the pseudo-first-order rate constant and t is the photodegradation time (min).

The kinetic parameter results are listed in Table 1. The k_{obs} values were determined by the linear plot of $\ln(C_t/C_0)$ and irradiation time (t min). Notably, $t_{50\%}$ (=0.693/k_{obs}) listed in Table 1 is an important parameter that represents the half-life time corresponding to 50% degradation of the initial humic acid concentration [16]. The determined R^2 values in the studied range of humic acid concentrations were high; thus, the photocatalytic reaction of the humic acid degradation using $FeNi_3/SiO_2/TiO_2$ MNCPs obeys a pseudo-first-order reaction. Moreover, the highest k_{obs} value was observed at an initial humic acid concentration of 5 mg/L, indicating the highest photocatalytic degradation efficiency of humic acid was obtained at this concentration value. This result is comparable with the findings of studies on the effect of initial concentration [40]. However, the negligibility of the mass transfer should be examined in future studies [41,42].

Table 1
Kinetic analysis for photocatalytic humic acid degradation

C_0	k_{obs} (min^{-1})	R^2	$t_{50\%}$ (min)
2	2.2×10^{-3}	0.9405	315
5	4.1×10^{-3}	0.9593	169.02
10	3.2×10^{-3}	0.9493	216.6
15	2.9×10^{-3}	0.9409	238.96

3.5. Regeneration and recycling study

The reusability of a catalyst is an important factor related to the cost of the treatment system. Therefore, the recyclability of the $FeNi_3/SiO_2/TiO_2$ MNCPs was tested for six consecutive photocatalytic degradation cycles under optimal conditions. At the end of each photocatalytic cycle, the $FeNi_3/SiO_2/TiO_2$ MNCP sample was withdrawn from the aqueous solution using a magnet, rinsed with ethanol and deionized water to remove the adsorbed humic acid molecules, dried in a vacuum oven at 80°C for 3 h, and then reused in the next photocatalytic degradation cycle. Fig. 9 shows that the $FeNi_3/SiO_2/TiO_2$ MNCPs used for the photocatalytic degradation of humic acid can be successfully recycled for six consecutive photocatalytic cycles. In this context, it was found that there was only a 3.9% reduction in the humic acid removal efficiency from the 1st to 6th cycles. This removal efficiency reduction may be due to a loss of photocatalytic ability due to separation, filtration, and washing processes. In addition, the reduction in $FeNi_3/SiO_2/TiO_2$ MNCPs per recycling cycle was negligible. From this experiment, it can be concluded that the $FeNi_3/SiO_2/TiO_2$ MNCPs have high reusability in the photocatalytic process of humic acid degradation.

4. Conclusion

$FeNi_3/SiO_2/TiO_2$ MNCPs were prepared and used as a photocatalytic agent to eliminate humic acid from contaminated solutions under solar light irradiation. Characterization analysis revealed that the $FeNi_3/SiO_2/TiO_2$ MNCPs possess unique practical properties and a high potential for application as an efficient photocatalyst. However, the optical properties of the synthesized nanocomposite catalyst should be tested in future studies. The solar light-photocatalytic process of the $FeNi_3/SiO_2/TiO_2$ MNCPs showed an excitation of the TiO_2 (shell layer) band level from the base to the CB level, leading to the generation of highly reactive $^{\bullet}O_2^-$ and ^-OH radicals. The generation of these radicals led to the oxidation of humic acid molecules into non-toxic chemicals, carbon dioxide and water. The highest degradation efficiency (82.3%) was achieved at a pH of 3, the humic acid concentration of 5 mg/L, $FeNi_3/SiO_2/TiO_2$ MNCPs dose of 0.03 g/L, and solar light irradiation time of 120 min. The photocatalytic process within the tested range of humic acid concentrations followed pseudo-first-order reaction kinetics. As a result, the photocatalytic process using $FeNi_3/SiO_2/TiO_2$ MNCPs under solar light irradiation is a safe, eco-friendly, and efficient technology for humic acid degradation. In addition, the suggested

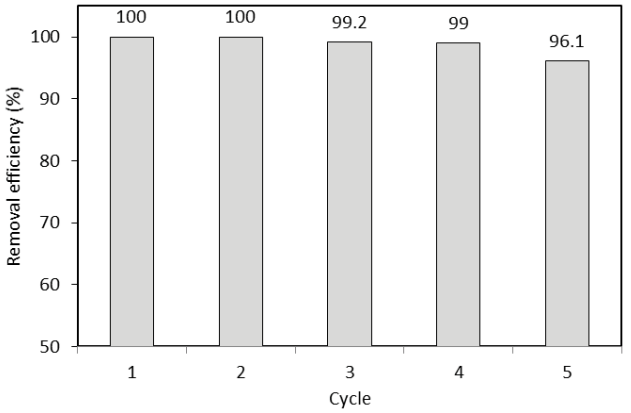

Fig. 9. Regeneration and recycling analysis of $FeNi_3/SiO_2/TiO_2$ MNCPs for humic acid degradation in the photocatalytic process.

treatment technology is believed to have potential applications in the tertiary units of wastewater treatment plants.

Acknowledgments

This work is the result of the dissertation approved by the Vice-Chancellor for Research and Technology/Birjand University of Medical Sciences, under the research-approval code: 455617. The authors are greatly indebted to the research laboratory staff of the Public Health School/Birjand University of Medical Sciences for help in completing this research.

References

[1] M. Qiu, B. Hu, Z. Chen, H. Yang, L. Zhuang, X. Wang, Challenges of organic pollutant photocatalysis by biochar-based catalysts, Biochar, 3 (2021) 117–123.
[2] M. Hao, M. Qiu, H. Yang, B. Hu, X. Wang, Recent advances on preparation and environmental applications of MOF-derived carbons in catalysis, Sci. Total Environ., 760 (2021) 143333, doi: 10.1016/j.scitotenv.2020.143333.
[3] A. Bhatnagar, M. Sillanpää, Removal of natural organic matter (NOM) and its constituents from water by adsorption–a review, Chemosphere, 166 (2017) 497–510.
[4] N. Turkten, I. Natali Sora, A. Tomruk, M. Bekbolet, Photocatalytic degradation of humic acids using $LaFeO_3$, Catalysts, 8 (2018) 630, doi: 10.3390/catal8120630.
[5] R. Al-Rasheed, D.J. Cardin, Photocatalytic degradation of humic acid in saline waters. Part 1. Artificial seawater: influence of TiO_2, temperature, pH, and air-flow, Chemosphere, 51 (2003) 925–933.
[6] C. Li, Y. Dong, D. Wu, L. Peng, H. Kong, Surfactant modified zeolite as adsorbent for removal of humic acid from water, Appl. Clay Sci., 52 (2011) 353–357.
[7] B. Bolto, D. Dixon, R. Eldridge, Ion exchange for the removal of natural organic matter, React. Funct. Polym., 60 (2004) 171–182.
[8] M.H. Ehrampoush, M. Taghi, T. Jasemizad, M. Askarshahi, Evaluation of the efficiency of electron beam irradiation for removal of humic acid from aqueous solutions, Tolooebehdasht, 16 (2017) 47–55.
[9] X.Z. Li, C.M. Fan, Y.P. Sun, Enhancement of photocatalytic oxidation of humic acid in TiO_2 suspensions by increasing cation strength, Chemosphere, 48 (2002) 453–460.
[10] M.Z. Pedram, M. Kazemeini, M. Fattahi, A. Amjadian, A physicochemical evaluation of modified HZSM-5 catalyst utilized for production of dimethyl ether from methanol, Pet. Sci. Technol., 32 (2014) 904–911.
[11] U.I. Gaya, A.H. Abdullah, Heterogeneous photocatalytic degradation of organic contaminants over titanium dioxide: a review of fundamentals, progress and problems, J. Photochem. Photobiol., C, 9 (2008) 1–12.
[12] S.M. Rahimi, F.S. Arghavan, A. Othmani, N. Nasseh, Magnetically recoverable nickel ferrite coated with CuS nanocomposite for degradation of metronidazole in photocatalytic and photo-Fenton like processes, Int. J. Environ. Anal. Chem., (2020) 1–21, doi: 10.1080/03067319.2020.1817420.
[13] X. Liu, R. Ma, L. Zhuang, B. Hu, J. Chen, X. Liu, X. Wang, Recent developments of doped g-C_3N_4 photocatalysts for the degradation of organic pollutants, Crit. Rev. Env. Sci. Technol., 51 (2021) 751–790.
[14] R. Yuan, B. Zhou, X. Zhang, H. Guan, Photocatalytic degradation of humic acids using substrate-supported Fe^{3+}-doped TiO_2 nanotubes under UV/O_3 for water purification, Environ. Sci. Pollut. Res. Int., 22 (2015) 17955–17964.
[15] L. Yao, H. Yang, Z. Chen, M. Qiu, B. Hu, X. Wang, Bismuth oxychloride-based materials for the removal of organic pollutants in wastewater, Chemosphere, 273 (2021) 128576, doi: 10.1016/j.chemosphere.2020.128576.
[16] N. Nasseh, T.J. Al-Musawi, M.R. Miri, S. Rodriguez-Couto, A. Hossein Panahi, A comprehensive study on the application of $FeNi_3$@SiO_2@ZnO magnetic nanocomposites as a novel photo-catalyst for degradation of tamoxifen in the presence of simulated sunlight, Environ. Pollut., 261 (2020) 114127, doi: 10.1016/j.envpol.2020.114127.
[17] M.-H. Baek, J.-S. Hong, J.-W. Yoon, J.-K. Suh, Photocatalytic degradation of humic acid by Fe-supported on spherical activated carbon with enhanced activity, Int. J. Photoenergy, 2013 (2013) 296821, doi: 10.1155/2013/296821.
[18] M.A. Nasseri, S.M. Sadeghzadeh, A highly active $FeNi_3$–SiO_2 magnetic nanoparticles catalyst for the preparation of 4H-benzo[b]pyrans and Spirooxindoles under mild conditions, J. Iran. Chem. Soc., 10 (2013) 1047–1056.
[19] A. Garmroudi, M. Kheirollahi, S.A. Mousavi, M. Fattahi, E.H. Mahvelati, Effects of graphene oxide/TiO_2 nanocomposite, graphene oxide nanosheets and Cedr extraction solution on IFT reduction and ultimate oil recovery from a carbonate rock, Petroleum, (2020), (in Press).
[20] M. Khodadadi, T.J. Al-Musawi, H. Kamani, M.F. Silva, A.H. Panahi, The practical utility of the synthesis $FeNi_3$@SiO_2@TiO_2 magnetic nanoparticles as an efficient photocatalyst for the humic acid degradation, Chemosphere, 239 (2020) 124723, doi: 10.1016/j.chemosphere.2019.124723.
[21] T. Komine, M. Nakagawa, Fundamental analysis for visible-light communication system using LED lights, IEEE Trans. Consum. Electron., 50 (2004) 100–107.
[22] T. Kozacki, M. Chlipala, Color holographic display with white light LED source and single phase only SLM, Opt. Express, 24 (2016) 2189–2199.
[23] M. Khodadadi, M.H. Ehrampoush, A. Allahresani, M.T. Ghaneianc, M.H. Lotfi, A. Mahvi, $FeNi_3$@SiO_2 magnetic nanocomposite as a highly efficient Fenton-like catalyst for humic acid adsorption and degradation in neutral environments, Desal. Water Treat., 118 (2018) 249–267.
[24] M. Khodadadi, M.H. Ehrampoush, M.T. Ghaneian, A. Allahresani, A.H. Mahvi, Synthesis and characterizations of $FeNi_3$@SiO_2@TiO_2 nanocomposite and its application in photocatalytic degradation of tetracycline in simulated wastewater, J. Mol. Liq., 255 (2018) 224–232.
[25] A. Mohseni-Bandpei, A. Eslami, H. Kazemian, M. Zarrabi, T.J. Al-Musawi, A high density 3-aminopropyltriethoxysilane grafted pumice-derived silica aerogel as an efficient adsorbent for ibuprofen: characterization and optimization of the adsorption data using response surface methodology, Environ. Technol. Innovation, 18 (2020) 100642, doi: 10.1016/j.eti.2020.100642.
[26] B. Paul, V. Parashar, A. Mishra, Graphene in the Fe_3O_4 nanocomposite switching the negative influence of humic acid coating into an enhancing effect in the removal of arsenic from

water, Environ. Sci.: Environ. Sci. Water Res. Technol., 1 (2015) 77–83.
[27] B. Akbari-Adergani, M.H. Saghi, Removal of dibutyl phthalate from aqueous environments using a nanophotocatalytic Fe, Ag-ZnO/VIS-LED system: modeling and optimization, Environ. Technol., 39 (2018) 1566–1576.
[28] F. Saadati, H. Aghajanloo, S. Piri, Preparation and characterization of nanoporous clay and its application as an effective catalyst in the Friedel-Crofts acylation of aromatic rings, J. Appl. Res. Chem., 11 (2017) 15–22.
[29] M. Khodadadi, M.H. Saghi, N.A. Azadi, S. Sadeghi, Adsorption of chromium VI from aqueous solutions onto nanoparticle sorbent: Chitozan-Fe-Zr, Majallahi Danishgahi Ulumi Pizishkii Mazandaran, 26 (2016) 70–82.
[30] E. Bazrafshan, T.J. Al-Musawi, M.F. Silva, A.H. Panahi, M. Havangi, F.K. Mostafapur, Photocatalytic degradation of catechol using ZnO nanoparticles as catalyst: optimizing the experimental parameters using the Box–Behnken statistical methodology and kinetic studies, Microchem. J., 147 (2019) 643–653.
[31] S.G. Rashid, M.A. Gondal, A. Hameed, M. Aslam, M.A. Dastageer, Z.H. Yamani, D.H. Anjum, Synthesis, characterization and visible light photocatalytic activity of Cr^{3+}, Ce^{3+} and N co-doped TiO_2 for the degradation of humic acid, RSC Adv., 5 (2015) 32323–32332.
[32] G.H. Safari, M. Hoseini, M. Seyedsalehi, H. Kamani, J. Jaafari, A.H. Mahvi, Photocatalytic degradation of tetracycline using nanosized titanium dioxide in aqueous solution, Int. Environ. Sci. Technol., 12 (2015) 603–616.
[33] V. Oskoei, M.H. Dehghani, S. Nazmara, B. Heibati, M. Asif, I. Tyagi, S. Agarwal, V.K. Gupta, Removal of humic acid from aqueous solution using UV/ZnO nano-photocatalysis and adsorption, J. Mol. Liq., 213 (2016) 374–380.
[34] F.S. Arghavan, A. Hossein Panahi, N. Nasseh, M. Ghadirian, Adsorption-photocatalytic processes for removal of pentachlorophenol contaminant using $FeNi_3/SiO_2/ZnO$ magnetic nanocomposite under simulated solar light irradiation, Environ. Sci. Pollut. Res., 28 (2021) 7462–7475.
[35] J.-K. Yang, S.-M. Lee, Removal of Cr(VI) and humic acid by using TiO_2 photocatalysis, Chemosphere, 63 (2006) 1677–1684.
[36] B. Akbari-Adergani, M. Saghi, A. Eslami, A. Mohseni-Bandpei, M. Rabbani, Modelling and optimization of a nanophotocatalytic process using Fe, Ag-ZnO under visible LED irradiation for dibutyl phthalate removal from aqueous environments, Environ. Technol., 39 (2017) 1–31.
[37] X. Li, D. Liu, S. Song, H. Zhang, $Fe_3O_4@SiO_2@TiO_2@Pt$ hierarchical core–shell microspheres: controlled synthesis, enhanced degradation system, and rapid magnetic separation to recycle, Cryst. Growth Des., 14 (2014) 5506–5511.
[38] N. Nasseh, F.S. Arghavan, N. Daglioglu, A. Asadi, Fabrication of novel magnetic $CuS/Fe_3O_4/GO$ nanocomposite for organic pollutant degradation under visible light irradiation, Environ. Sci. Pollut. Res., 28 (2021) 19222–19233.
[39] J. Rashid, M.A. Barakat, Y. Ruzmanova, A. Chianese, $Fe_3O_4/SiO_2/TiO_2$ nanoparticles for photocatalytic degradation of 2-chlorophenol in simulated wastewater, Environ. Sci. Pollut. Res., 22 (2015) 3149–3157.
[40] D. Dimitrakopoulou, I. Rethemiotaki, Z. Frontistis, N.P. Xekoukoulotakis, D. Venieri, D. Mantzavinos, Degradation, mineralization and antibiotic inactivation of amoxicillin by UV-A/TiO_2 photocatalysis, J. Environ. Manage., 98 (2012) 168–174.
[41] M. Fattahi, M. Kazemeini, F. Khorasheh, A. Rashidi, An investigation of the oxidative dehydrogenation of propane kinetics over a vanadium–graphene catalyst aiming at minimizing of the COx species, Chem. Eng. Sci., 250 (2014) 14–24.
[42] L. Vafajoo, F. Khorasheh, M.H. Nakhjavani, M. Fattahi, Kinetic parameters optimization and modeling of catalytic dehydrogenation of heavy paraffins to olefins, Pet. Sci. Technol., 32 (2014) 813–820.

Supplementary information

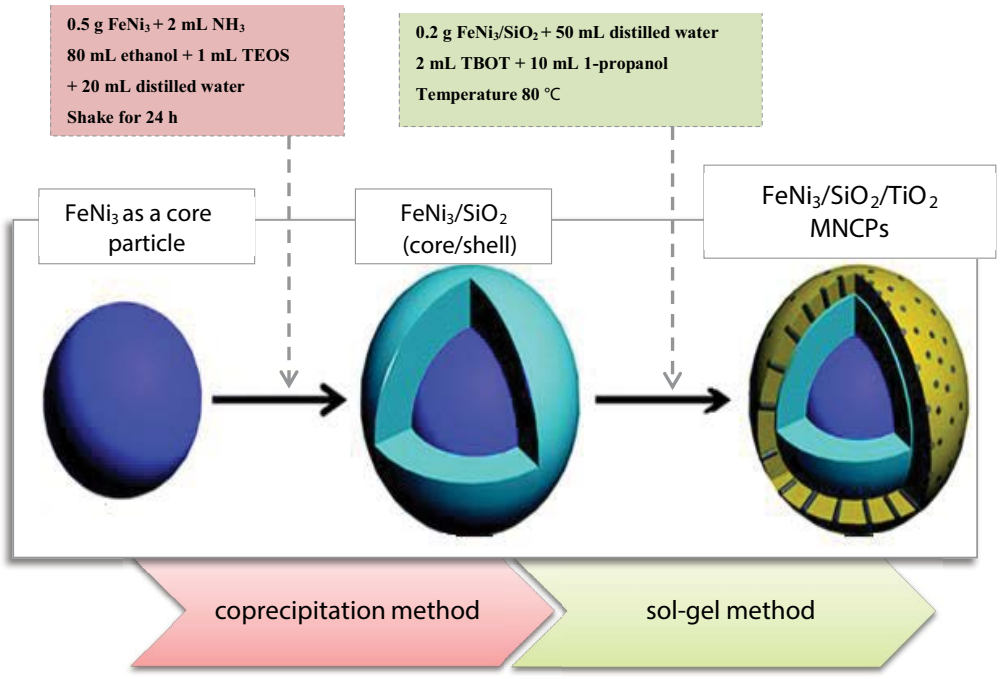

Fig. S1. Experimental methodology was used to synthesize $FeNi_3/SiO_2/TiO_2$ MNCPs, where TEOS and TBOT are tetraethyl orthosilicate and tetrabutyl orthotitanate, respectively.

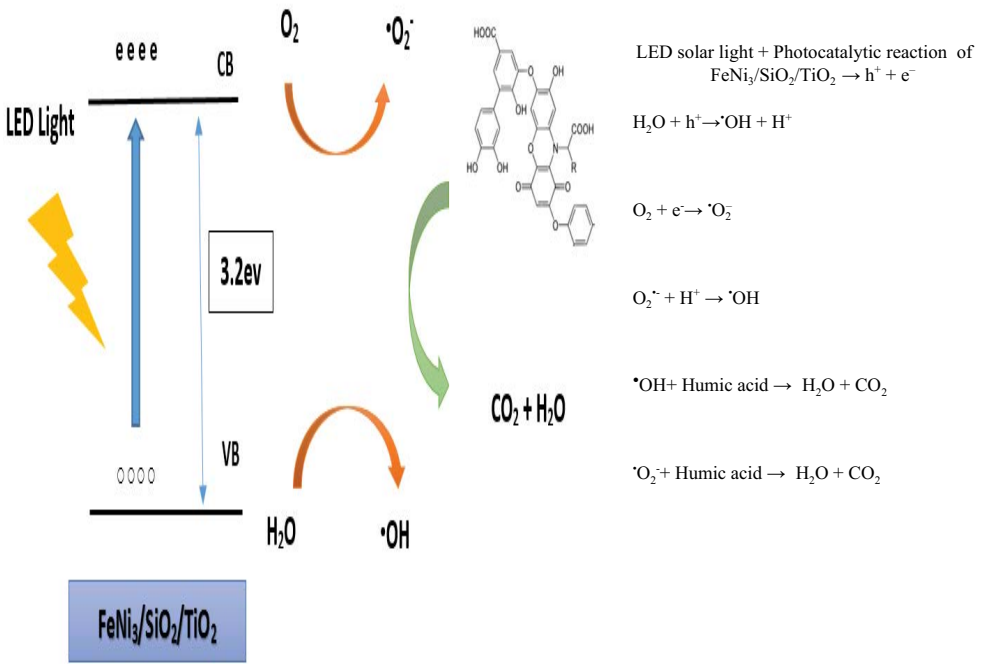

Fig. S2. Mechanism and chemical reactions of the photocatalytic degradation of humic acid